THE JOURNAL OF PHYSICAL CHEMISTRY B

ARTICLE

pubs.acs.org/JPCB

Evidence for the Presence of Two Conformations of the Heme a_3-Cu_B Pocket of Cytochrome caa_3 from *Thermus thermophilus*

Andrea Pavlou,[†] Tewfik Soulimane,[‡] and Eftychia Pinakoulaki*[,†]

[†]Department of Chemistry, University of Cyprus, P.O. Box 20537, 1678 Nicosia, Cyprus

[‡]Chemical and Environmental Sciences Department and Materials & Surface Science Institute, University of Limerick, Limerick, Ireland

ABSTRACT: Resonance Raman (RR) and "light" minus "dark" Fourier transform infrared (FTIR) difference spectra are reported for the CO-bound caa_3 oxidase from *Thermus thermophilus*. Two Fe−CO stretching modes at 518 and 507 cm^{-1}, the Fe−C−O bending mode at 570 cm^{-1}, and three C−O modes of heme a_3 at 1958, 1967, and 1973 cm^{-1} have been identified in the RR and FTIR spectra, respectively. The FTIR "light" minus "dark" spectrum indicates the formation of Cu_BCO as revealed by its ν(CO) at 2060/2065 cm^{-1}. We assign the bands at 518 (ν_{Fe-CO}) and 1967/1973 cm^{-1} (ν_{C-O}) as the α-conformation. We also assign the bands at 507 and 1958 cm^{-1} (ν_{C-O}) as originating from the β-conformation of the enzyme. A frequency upshift of the heme a_3 Fe-His mode is observed subsequent to CO photolysis from 209 cm^{-1} in the equilibrium deoxy enzyme to 214 cm^{-1} in the photoproduct. The caa_3 data, distinctly different from those of ba_3 oxidase, are discussed in terms of the coupling of the α- and β-conformations that occur in heme-copper oxidases with catalytic function. The dynamics between the heme a_3 and heme a propionates as revealed by the perturbation of the bending vibrations δ_{prop} of hemes a and a_3 at 385 and 392 cm^{-1}, respectively, induced upon CO binding to heme a_3 is discussed in terms of the protonic connectivity between the heme a ring-D propionate/Arg site with that of the heme a_3 ring-D propionate-H_2O site that leads to the highly conserved in the heme-copper oxidases water pool.

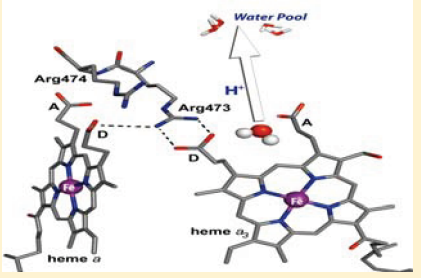

INTRODUCTION

Cytochromes caa_3 and ba_3 from *Thermus thermophilus* serve as the terminal heme-copper oxidases in the thermophilic Gram-negative eubacterium *T. thermophilus* HB8 (ATCC27634).[1] Both enzymes have been of much interest due to their unique catalytic properties.[2] They reduce oxygen to water and nitric oxide to nitrous oxide under anaerobic conditions.[3] The heme-copper caa_3 oxidase contains a mixed-valence [$Cu_A^{1.5+}$-$Cu_A^{1.5+}$] homodinuclear copper complex, two low-spin hemes (*a*- and *c*-type), and a binuclear center that consists of Cu_B and heme a_3.[1,2] The *a*-type heme in caa_3 contains a hydrophobic hydroxyethyl-geranylgeranyl-group instead of a hydroxyethylfarnesyl chain found in most bacterial and eukaryotic aa_3 oxidases.[1] Given that caa_3 is a member of the heme-copper oxidase family, it is essential to learn its structure and function and thus understand its dual function in catalyzing the reduction of both O_2 and NO.[4−12]

The molecular mechanisms of the caa_3 oxidase is expected to be similar to its counterpart ba_3 oxidase and to other distantly related heme-copper oxidase with respect to the oxygen and nitric oxide chemistry since the central features of the active site are similar and the catalyzed chemical reactions identical.[8−10] On the basis of the available crystal structure of heme-copper oxidases, it has been suggested that the proton pathway starts at the cytoplasmic site and through the heme a_3 propionates leads directly to accumulation of water molecules.[13−15] In the crystallographic structure of aa_3 (*P. denitrificans*) the propionate groups attached to the D-rings of heme a and a_3 form strong H-bonds with Arg473.[14] On this line, the propionates have been postulated to play critical roles in both electron transfer and proton translocation events.[15] Given the complexity of these processes, it is essential to determine what structural changes occur upon ligand binding to the catalytic center that lead to the highly conserved catalytic center and to new issues regarding the properties and dynamics of the heme a and a_3 propionates upon ligand binding with respect to proton motion and the proton exit channel.

Structural information on the heme-Cu_B center in bacterial oxidases has been determined from studies of their CO-bound form.[16−24] In addition to revealing insights concerning the geometry of the bound ligand, the identity of the proximal ligand, as well as the interactions between the bound CO and the surrounding residues in the heme pocket, CO photodissociation and recombination studies have been very powerful for studying the conformational and structural changes as well as the kinetic properties of transient species.[25−29] The Fourier transform infrared (FTIR) and step-scan time-resolved FTIR spectra of caa_3 oxidase at room temperature have revealed several structural characteristics of the heme-copper pocket.[30] A major C−O mode of heme a_3 at 1958 cm^{-1} and two additional modes at 1967 and 1975 cm^{-1} were identified at room temperature and remained unchanged in H_2O/D_2O exchange suggesting the presence of an a_3-type heme of a β-form. The time-resolved FTIR data indicated that the transient Cu_B^{1+}-CO complex is formed at room

Received: April 10, 2011
Revised: August 18, 2011
Published: August 19, 2011

temperature as revealed by the CO stretching mode at 2062 cm^{-1} indicating that Cu_B is in the α-form. Moreover, it was found that the dissociation of the transient Cu_B^{1+}-CO complex is biphasic and occurs with $t(1)_{1/2}$ of 30 μs (fast phase, 35%) and with $t(2)_{1/2}$ of 19.1 ms (slow phase, 65%), and the rebinding to heme a_3 occurs with $t_{1/2}$ of 20.3 ms. It was concluded that the dissociation of CO from Cu_B^{1+} in the slow-phase is the rate-limiting step for recombination of CO to heme a_3 and that the long-lived Cu_B^{1+}-CO complex is expected to interfere in the flow-flash oxygenation experiment. Although the kinetic data showed that there are two distinct populations of the enzyme with different rates of dissociation of the Cu_B^{1+}-CO complex, it was proposed that the population (35%) of the enzyme with the fast phase is not substantial to allow uninhibited access of O_2 to the active site and, thus, create favorable conditions for the flow-flash experiment. Similar conclusions were reported for the ba_3 oxidase.[25]

Resonance Raman (RR) spectroscopy has been applied to the study of heme-copper oxidases and has been found to be a powerful tool in probing the bonds of the hemes and the bonds between the heme Fe and the bound proximal- and distal ligands.[31−36] RR studies of the caa_3 revealed strong similarities of the proximal ligation and heme environments with those found in other heme-copper oxidases.[4] In the low-frequency region of the RR spectrum of fully reduced caa_3, a single vibration at 213 cm^{-1} has been assigned to the iron-histidine stretch of heme a_3 in the equilibrium deoxy form, while two modes at 193 and 210 cm^{-1} in heme a_3 of ba_3 oxidase that is known from crystallographic studies to be H-bonded to Gly359 have been assigned to ν(Fe-His).[24−36] Furthermore, by following the assignments of Gerscher et al. and those originally reported by Ching et al., among other low-frequency vibrations the bending vibrations δ_{prop} of hemes a and a_3 propionates at 385 and 393 cm^{-1}, respectively, were identified.[4,5]

To provide a better understanding of the existing conformers in caa_3 oxidase and the possible heme-protein coupling upon ligand binding (CO) to heme a_3, we have used RR and "light" minus "dark" FTIR difference spectra of the heme-bound CO, which is used as a spectroscopic antenna, to probe the original conformers in the heme-Cu_B binuclear center. Our results indicate that, despite the presence of a single proximal iron-histidine mode in the ligand-free, equilibrium deoxy form of the enzyme, in the caa_3-bound CO complex, two stretching modes and a single bending mode are identified as ν(Fe-CO) at 518 and 507 cm^{-1} and δ(Fe-C-O) at 570 cm^{-1}. The data also demonstrate, in addition to the presence of a photolabile β-form with characteristic Fe−CO and C−O stretching modes at 507 and 1958 cm^{-1}, respectively, the presence of a photolabile α-form. The latter form of caa_3 has characteristic Fe−CO and C−O stretching modes at 518 and 1967/1973 cm^{-1}. The analysis of the data also reveals that the binding of CO to heme a_3 is dynamically linked to structural changes in the environment of the propionates (COOH) of heme a_3 ($\delta_{CbC\alpha C\beta}$ = 392 cm^{-1}) and heme a ($\delta_{CbC\alpha C\beta}$ = 385 cm^{-1}). The photoproduct spectrum obtained upon CO-photolysis indicates an upshift by 5 cm^{-1} of the Fe-His frequency from 209 cm^{-1} in the equilibrium enzyme to 214 cm^{-1}. The observation that there are no changed in the vibrational modes such as ν_8 (327 cm^{-1} in heme a_3 and 346 cm^{-1} in heme a) and δ_{prop} in the photoproduct which has contributions from bending motions of peripheral substituents illustrates that heme−protein interactions occur through the heme Fe−His bond. The analysis of the "light" minus "dark" FTIR also reveals the presence of the CO stretching frequencies at 2060/2065 cm^{-1} of the Cu_B-CO complex suggesting that Cu_B is in the α-form at room temperature. The α-form of the Cu_B-CO complex in conjunction with the α- and β-forms of the heme a_3 unambiguously establishes the vibrational characteristics of the heme−copper moiety in caa_3-oxidase. Moreover, the dynamics of the ligation reactions at the binuclear center and the environment between heme a_3 and heme a propionates are discussed.

EXPERIMENTAL METHODS

The purification of caa_3 and ba_3 oxidases was followed according to procedures in refs 4 and 30. The concentration of caa_3 was determined from reduced-oxidized enzyme using an absorption coefficient ε_{605} = 11.7 mM^{-1} cm^{-1}. For the FTIR experiments, dithionite reduced samples (~500 μM) were exposed to 1 atm of CO in an anaerobic cell to prepare the carbonmonoxy adduct and loaded anaerobically into an FTIR cell with CaF_2 windows and a 0.025 mm spacer. CO gas was obtained from Linde Gas, and isotopic CO ($^{13}C^{18}O$) was purchased from Isotec. FTIR spectra were obtained with a Bruker Vertex 70 spectrometer equipped with a liquid-nitrogen-cooled mercury cadmium telluride detector. The FTIR spectra were obtained as difference spectra, using the buffer as a background, and each spectrum is the average of 500 scans. The photolysis light was provided by a Coherent Cube continuous wave 447 nm diode laser, and the incident power on the sample was 30 mW. The light-minus-dark difference spectra are the average of 4000 scans. Optical absorbance spectra were recorded before and after the FTIR measurements to access sample stability with a Shimadzu UV-1700 UV−visible spectrometer. The resonance Raman experiments were carried out with continuous wave (c.w) 426 nm excitation, as described previously.[34] Approximately 40 μL of a 50 μM enzyme solution in 20 mM *N*-(2-hydroxyethyl)piperazine-*N*′-ethanesulfonic acid (HEPES), pH 7.4 containing 0.05% dodecyl β-D-maltoside was placed in a rotating (4000−6000 rpm) quartz Raman cell to minimize local heating. The sample cells are custom-designed and can be used for recording both the resonance Raman and optical absorption spectra. Frequency shifts in the Raman spectra were calibrated with toluene. The accuracy of the Raman shifts is about ±2 cm^{-1} for absolute shifts and about ±1 cm^{-1} for relative shifts. The incident laser power was 1−2 mW, and the total accumulation time was 20−30 min for each spectrum.

RESULTS

Figure 1 shows the low-frequency RR spectra of CO-bound caa_3 at neutral pH obtained with continuous wave 426 nm excitation, in which resonances from heme a, heme a_3, and heme a_3-CO are enhanced.[4] Raman bands in the 200−700 cm^{-1} range include, in addition to vibrations of the porphyrin macrocycles of heme a and heme a_3, heme-Fe-ligand motions along the axis normal to the heme. No contributions from heme c are observed with 426 nm excitation. Figure 1 depicts the low-frequency RR data of reduced (trace A), the ^{12}CO- (trace B), and $^{13}C^{18}O$-bound (trace C) forms and the photostationary ^{12}CO-bound spectrum of the fully reduced enzyme (trace D). The addition of CO to the fully reduced enzyme causes the disappearance of the 209 cm^{-1} mode which was tentatively assigned to a ν(Fe-His) and the appearance of a mode at 232 cm^{-1}. This is a common behavior of a six-coordinated His-heme Fe-CO complex in heme-copper oxidases.[22−24] Significant frequency shifts and intensity changes are also observed in the modes at 346 (ν_8 of heme a), 327 (ν_8 of

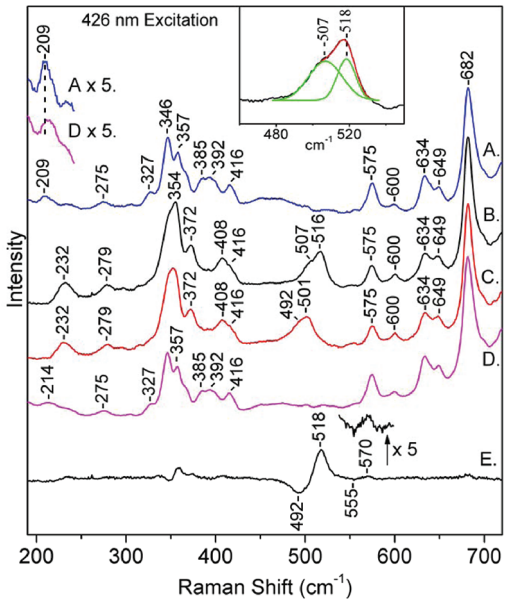

Figure 1. Resonance Raman spectra of cytochrome caa_3 from *Thermus thermophilus* in the reduced (trace A), reduced-$^{12}C^{16}O$ bound (trace B), reduced-$^{13}C^{18}O$ bound (trace C), and photodissociated reduced-$^{12}C^{16}O$ bound (trace D) states. The difference spectrum $^{12}C^{16}O-^{13}C^{18}O$ (trace E) is also included. The excitation continuous wave laser wavelength was 426 nm, and the accumulation time was 30 min for each spectrum. The inset shows the curve fitting results in the 480−540 cm^{-1} spectral region for trace B; the green lines are the band fitting components, and the red line is the sum of the component bands.

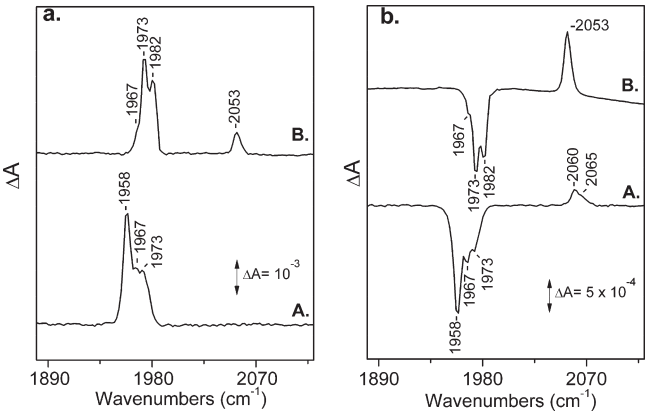

Figure 2. Panel a: FTIR spectra of cytochrome caa_3-CO (trace A) and cytochrome ba_3-CO (trace B) adducts from *T. thermophilus*. Panel b: Light-minus-dark FTIR difference spectra of cytochrome caa_3-CO (trace A) and cytochrome ba_3-CO (trace B) adducts at ambient temperature. The enzyme concentration was 0.5 mM, and the path length was 25 μm. The spectral resolution was 4 cm^{-1}.

heme a_3), 357 (ν_{50} of heme *a*), 385 (bending vibration of heme *a* propionates δ_{prop}), and 392 cm^{-1} (bending vibration of heme a_3 propionates δ_{prop}), and negligible changes are observed in the intensities of the modes in the 575−700 cm^{-1} range upon CO binding to heme a_3. Specifically, the δ_{prop} of heme a_3 at 392 cm^{-1} has lost all of its intensity, and unexpectedly, the same has occurred for the δ_{prop} of heme *a*. This is the first evidence of coupling between the heme *a* and a_3 propionates upon ligand (CO) binding to heme a_3. The spectrum of the $^{13}C^{18}O$-bound fully reduced enzyme is depicted in trace C, and the frequencies of all modes are the same with those observed in the $^{12}C^{16}O$-bound spectrum with the exception of three modes that have carbon and oxygen isotopic sensitivity. The shifts are more evident in the difference spectrum (trace E) between the $^{12}C^{16}O$- and the $^{13}C^{18}O$-bound states. The inset shows the curve fitting results in the 480−540 cm^{-1} spectral region for trace B; the green lines are the band fitting components, and the red line is the sum of the component bands. The ν(Fe-CO) at 518 cm^{-1} (fwhm = 12 cm^{-1}) is similar to that found in the aa_3-type oxidases from *P. denitrificans*,[36] aa_3-600,[22] bovine heart,[37] and *Rhodobacter sphaeroides*.[17] The ν(Fe-CO) at 507 cm^{-1} (fwhm = 21 cm^{-1}) is very similar to that found in the ba_3 oxidase and 14 cm^{-1} higher than that of the β-from of *R. sphaeroides*.[17,21] In addition, the shift of the weak mode at 570−555 cm^{-1} appears in the isotope difference spectrum (trace E). This mode is attributed to the Fe−C−O bending mode and is 5−10 cm^{-1} lower than that of the aa_3-type oxidases.[37] The ratio of the intensity of the Fe−C−O bending mode to that of the Fe-CO stretching mode is I_δ/I_ν = 0.1. The high power spectrum of the CO-bound caa_3 obtained at higher laser power (4 mW) shows that the intensities of all CO-sensitive modes have diminished, indicating that the Fe-CO species are photolabile. In the RR spectrum of caa_3 the line detected at 210.6 cm^{-1} was tentatively assigned to ν(Fe-His).[4] The spectrum of the fully reduced enzyme (trace A) confirms the existence of a mode at 209 cm^{-1} and its absence, as expected, in both traces C and D. Trace C shows the photostationary RR spectrum of the CO-bound caa_3. All of the heme modes have the same frequencies as those found in the fully reduced enzyme with the exception of the 214 cm^{-1} mode that is upshifted by 5 cm^{-1} from its equilibrium position at 209 cm^{-1}. This observation confirms the assignment of the 209 cm^{-1} mode shown in trace A as the heme a_3 Fe-His mode (see below).

In Figure 2 (panel a, trace A) we present the FTIR spectra of the CO-bound cytochrome caa_3 complex at neutral pH at room temperature. For comparison, we have included the analogous spectra of cytochrome ba_3 (trace B). The spectra of the CO-bound forms of the enzyme exhibit a major peak at 1958 cm^{-1} and two peaks of similar intensity at 1967 and 1973 cm^{-1}. The spectrum of the ba_3 shown in trace B exhibits peaks at 1982, 1973, and 1967 cm^{-1} which have been attributed to different conformations of the heme Fe-CO complex (complex **B**) and 2053 cm^{-1} which represents CO binding to Cu_B^{1+} (complex **A**) in agreement with the spectra previously reported.[25] In panel b we present the "light" minus "dark" FTIR difference spectra of caa_3 (trace A) and ba_3 oxidases (trace B). Upon photolysis, CO is transferred from heme a_3 to Cu_B. The negative peaks in trace A arise from the photolyzed heme a_3-CO. The positive peaks that appear at 2060 and 2065 cm^{-1} are attributed to the C−O stretch (ν_{CO}) of Cu_B. The frequencies of the C−O mode in the photoproduct are similar to that found in the transient Cu_B^{1+}-CO complex at 2062 cm^{-1}, and its frequency, but not its intensity, is very similar to that obtained at 21 K.[6] In the aa_3-type oxidases, the frequencies of Cu_B^{1+}-CO at 2064 and 2042 cm^{-1} are associated with the α- and β-forms, respectively.[6,17] Therefore, the Cu_B^{1+}-CO complex in caa_3 with characteristic ν(CO) at 2060/2065 cm^{-1} is of the α-form, and the presence of the hydroxyethylgeranylgeranyl side chain has no effect on the vibrational properties of the bound CO to either the heme a_3 or Cu_B. In trace B the negative peaks arise from the photolyzed heme a_3-CO complex and the single positive peak at 2053 cm^{-1}

dx.doi.org/10.1021/jp2033356 |J. Phys. Chem. B 2011, 115, 11455–11461

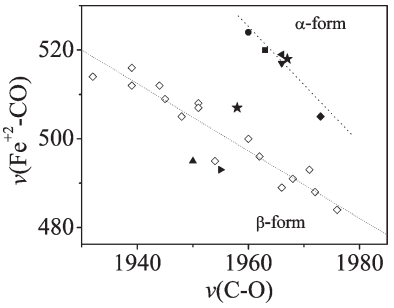

Figure 3. Correlation between frequencies of the Fe−CO versus C−O stretching modes for the α- and β-forms of heme-copper oxidases. (★) cytochrome caa_3 from *T. thermophilus* (this work), (♦) cytochrome ba_3 from *T. thermophilus*,[23] (▼) cytochrome aa_3 from *P. denitrificans*,[36] (■) cytochrome aa_3-600 from *B. subtilis*[22] and mammalian cytochrome *c* oxidase,[37] (◄) the α form of cytochrome aa_3 from *R. sphaeroides*,[17,21] (●) cytochrome bo_3 from *E. coli*,[20] (▲) cytochrome cbb_3 from *R. capsulatus*,[18] (►) the β form of cytochrome aa_3 from *R. sphaeroides*,[17,21] (◇) myoglobins, hemoglobins, and other heme-proteins with His proximal ligation.[17,18,21]

to Cu_B^{1+}-CO complex of ba_3 oxidase. A comparison of the data presented in panels a and b strongly indicates major differences in the ligand binding states between the caa_3 and the ba_3 oxidases.

DISCUSSION

We report here a detailed characterization of the heme pocket of the caa_3 oxidase and discuss our results with respect the dynamics of the His-Heme a_3 Fe···Cu_B moiety and the protein dynamics between the propionates of heme a_3 and a upon CO binding to heme a_3. Based on the ν_{Fe-CO} versus ν_{C-O} correlation of many heme Fe−Cu_B proteins, shown in Figure 3, we assign the CO-bound forms of the enzyme with bands at 518 (ν_{Fe-CO}) and 1967/1973 cm^{-1} (ν_{C-O}) as the α-conformation. We also assign the CO-bound form with frequencies at 507 (ν_{Fe-CO}) and 1958 cm^{-1} (ν_{C-O}) as originating from the β-conformation of the enzyme. When plotted on a ν_{Fe-CO} versus ν_{C-O} correlation curve, these frequencies fall on the line observed for heme proteins having histidine residue as their proximal ligand. This demonstrates that in caa_3 oxidase, the fifth ligand to the heme is the imidazole side chain of a histidine residue. The ligation of CO to Cu_B upon CO photolysis from heme a_3 uncouples the heme a_3-prop-heme a-prop interaction. The elucidation of the mode of ligand binding of caa_3 is important to exploit the protein environment that has been implicated in the catalytic properties of heme copper oxidase and also in the proton pumping mechanism of the enzyme.

Ligand Binding States of the His-Heme a_3 Fe···Cu_B Moiety. A confirmation of histidine as the proximal ligand is revealed from the analysis of the Fe^{2+}-CO complex. It is well-known that there is an inverse correlation between the frequencies of the ν_{Fe-CO} stretching modes and the frequencies of the ν_{C-O} stretching modes of heme proteins and heme model compounds.[17] This relation arises from the π-electron back-donation from the $d_\pi(d_{xz}, d_{yz})$ orbitals of Fe to the empty π^* orbitals of CO; the bond order between the Fe and CO increases as the bond order between the carbon and the oxygen atoms of CO decreases and vice versa. In the absence of the fifth ligand or depending on the nature of the proximal ligand, different correlation lines are observed due to differences in the charge on Fe that are reflected in the strength of the Fe−CO bond. Vibrational spectroscopy has been applied extensively to explore the factors that can influence the strength of the C−O bond in the heme Fe−CO Cu_B complexes, and thus, a large body of data is available.[8,16,17,21,23,33,37] For instance, distal effects involving the interaction of Cu_B could alter the conformation of the Fe−C−O group from its preferred symmetry into a bent or tilt conformation, thereby raising the C−O frequency. Also, the strength of the proximal histidine H-bonding interaction affects the strength of both the Fe−C and the C−O bonds that are further influenced by the Cu_B distal environment.[22,23,36] The Fe-His vibration of heme a_3 in caa_3 has a frequency at 209 cm^{-1},[4] which is close to those found in other aa_3 type oxidases and to the high-frequency Fe-His (193 and 208 cm^{-1}) conformer of ba_3.[7,8,35]

In heme-copper oxidases, the α-form represents a ligand binding conformation of the enzyme in which the frequencies of ν(Fe-CO) and ν(CO) lie off the correlation curve for heme proteins with a trans histidine ligand.[17,21] In the β-form the frequencies are placed on the correlation curve,[22] and in the γ-conformation Cu_B is moved closer to the CO-bound heme a_3; thereby the Fe−C−O moiety is further distorted from its preferred symmetry in the α-form.[36] Although equivalent differences have not been detected in other coordination and oxidation states of the heme-copper oxidases, the position of Cu_B with respect to the ligand bound to the heme and not to the heme directly determines very specific ligand binding states. Consequently, there are such specific conformational states which in turn control enzyme activity. A comparison of the caa_3 oxidase to ba_3 oxidase may provide the means to identify conserved structural features, which can be assumed to be involved in basic functions common to both enzymes. In contrast, dissimilarities between these enzymes are likely to be involved in the fine-tuning to specific needs required by differences in the structure of binuclear heme-Cu_B center. Recently, it was reported that the contribution of Cu_B to the split of the heme Fe-CO vibrations (α-, β-, and γ-forms) is not the result of changes in the ligation and or protonation states of its ligands but rather to a global protein conformational change in the vicinity of Cu_B that affects the distance between the two metal centers.[25]

The sensitivity of CO to electrostatic interactions arises from its lone pair of electrons that is delocalized when CO is near charged groups. When the CO is near a negative charged group (Fe−C≡$O^{\delta+}$−X^-), the Fe−CO bond tends toward a single bond character, and the C−O bonds tend toward a triple bond character. On the other hand, when CO is near a near a positively charged group, the Fe═C═O-X^+ structure is stabilized in which the Fe−CO and C−O bonds have a double bond character.[38,39] In heme-copper oxidases the enchancement of the bending mode in the α-form is the result of steric forces which caused it to bent or tilted, and the Cu_B serves to lower its symmetry so that the δ(Fe−C−O) is enhanced.[17] RR spectra of heme model compounds have revealed that the intensity of the bending vibration is proportional to the sterically induced tilting of the CO away from the heme plane. It is expected that due to the large force constant the C−O stretching frequency is insensitive to geometry changes while the Fe-CO is very sensitive. In the bovine aa_3 oxidase the CO is tilted by 21° with respect to the heme plane.[40] The observed I_δ/I_ν (518 cm^{-1}) = 0.1 in caa_3 for the α-form is very low when compared to that found in heme a_3-Cu_B oxidases (I_δ/I_ν = 0.2−0.4). Of note, in ba_3 oxidase I_δ/I_ν = 0.3 which indicates strong interaction between the CO and the Cu_B.[23] Thus, Cu_B does not exert similar steric forces to Fe−C−O in caa_3 as those in ba_3 and aa_3-type oxidases, and

consequently Cu_B, as opposed in the majority of heme-copper oxidase in the α-form, has a weak effect in the formation of the α-form. In the absence of steric and polar interactions, we suggest that the strength of the proximal histidine H-bonding interaction affects the strength of the Fe−C and C−O bonds. This explanation finds support from the reported Fe−C−O and C−O frequencies of the α-form of ba_3 oxidase and the crystal structure where it has been shown that the distance from N_δ of His384 to the carbonyl of Gly359 (ba_3 *T. thermophilus* numbering) is 3.43 Å (H-bonding distance).[2]

Photodynamics of the CO-Conformers. The determination of the structures in the binuclear center upon CO binding and release is a complex process that involves ligand motion through the protein and extensive changes in the heme electronic structure and molecular conformation. The photodissociation/rebinding process remains an important problem that is central to elucidating the dynamics of heme-copper oxidases. In order to determine the molecular basis for the function of heme-copper oxidases it is necessary to understand the interactions between the heme-bound ligands and the residues in their distal environment. Ultimately, this should lead to an understanding of the ligand kinetic behavior and the active site(s) properties. The binding/release and photodynamics of CO to heme-copper oxidases proceeds according to Schemes 1 and 2.

In these schemes, k_1 and k_{-1} represent the reversible binding of CO to Cu_B, and k_2 is the first order transfer of CO from Cu_B to the heme Fe.[3,25,30,31] In the photodissociation of CO from fully reduced depicted in Scheme 2, the heme Fe-histidine vibration of ferrous deoxy heme a_3 is detected at 221 cm^{-1} following CO photolysis. In these experiments, the ν(Fe-His) vibration of ferrous deoxy heme a_3 in the bovine aa_3 oxidase was observed at 221 cm^{-1} and shifted to its 215 cm^{-1} equilibrium value as the relaxation proceeded, which was interpreted according to Scheme 2. The state denoted by an asterisk {His-Fe^{2+}}* represents a nonequilibrium heme a_3 state characterized by an upshifted Fe-His stretching vibration which, in the mammalian aa_3 oxidase, relaxes to the equilibrium reduced species at times >10 μs.[31] In the experiments reported here the continuous wave 426 nm laser photodissociates the bound ligand and produces Raman scattering from the photolysis product. The experimental data in Figure 1 show that the photosensitivity of the α- and β-forms produces, as measured by the light-induced generation of the {His-Fe^{2+}}*, a single instead of two ν(Fe-His). This is consistent with the fact that the hemepocket does not interconvert between two discrete geometries, that is, one that corresponds to the α-form and the other to the β-form. Rather the pocket evolves in a manner with a continuum of available geometries. We postulate that following the onset of CO rebinding there is a fairly large scale motion of the protein proximal pocket that arises from the variation in proximal histidine hydrogen bonding between transient and equilibrium species. Concurrently, by placing diffusional barriers and by removing steric restrictions directly adjacent to the heme a_3 Fe, the protein forces that ultimately produce an equilibrim Cu_B configuration fix the heme Fe-Cu_B distance to reproduce the α- and β-forms.

Evidence for Additional Heme a_3-Protein-Heme *a* Interactions. The propionate groups of heme *a* and heme a_3 in cytochrome oxidase have been postulated to mediate both the electron and the proton transfer in the enzyme and recently were reported.[41−43] In caa_3 the contribution of protonated and ionized carboxylic groups of the heme propionates has been demonstrated in the electrochemically induced FTIR difference spectra reported, previously.[44] In the crystallographic structures of cytochrome oxidases, the propionate groups attached to the D-rings of hemes *a* and a_3 form strong H-bonds with an Arg residue, as seen in Figure 4.[13,14] On this line, a reversible redox-state dependent dissociation of the prop-D/arginine salt bridge has been proposed to be triggered by the hydration of the heme a_3 ring-D propionate.[15] It has been suggested that the protonation of the arginine is transient and coupled to deprotonation of the arginine which releases its proton to a site above the heme groups.[15] In addition, a conserved water close to heme a_3 ring-D propionate, but always in the area between (2.2−2.8 Å) the ring-A and ring-D propionates of heme a_3, has been proposed to act as a possible proton carrier.[15] We propose that the CO-binding to heme a_3 associated changes in the $\delta_{CbC\alpha C\beta}$ = 385 cm^{-1} of heme *a* and $\delta_{CbC\alpha C\beta}$ = 392 cm^{-1} of heme a_3 modes of the propionate groups upon ligand binding to heme a_3 are a result of the perturbation in this H-bonding network between the ring-A and ring-D propio-

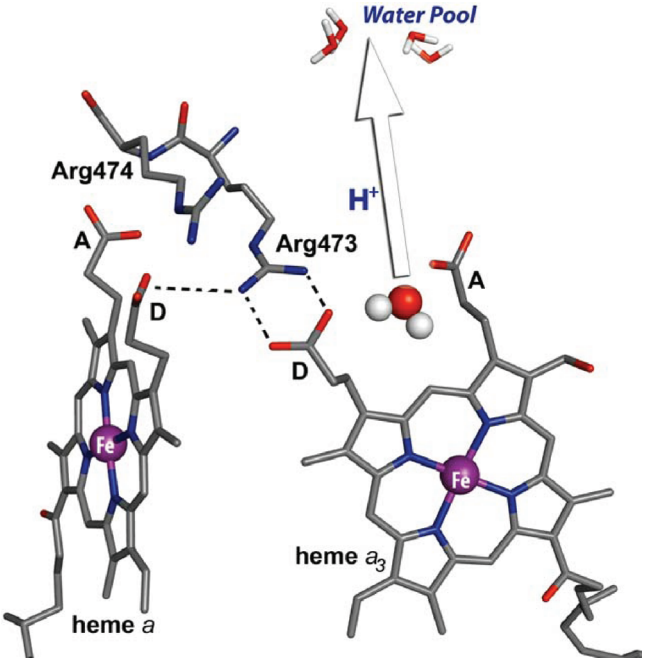

Figure 4. X-ray crystallographic structures of hemes *a* and a_3 of the active site of aa_3 cytochrome *c* oxidase from *P. denitrificans*.

Scheme 1

$$Fe^{2+}\,Cu_B^{1+} + CO \underset{k_{-1}}{\overset{k_1}{\rightleftharpoons}} Fe^{2+},\,Cu_B^{1+}\text{-}CO \underset{k_{-2}}{\overset{k_2}{\rightleftharpoons}} Fe^{2+}\text{-}CO,\,Cu_B^{1+}$$

A **B**

Scheme 2

$$\text{His-}Fe^{2+}\text{-}CO,\,Cu_B^{1+} \xrightarrow{h\nu} \{\text{His-}Fe^{2+}\}^*,\,Cu_B^{1+}\text{-}CO \rightarrow CO\ (sol.),\,Cu_B,\,\text{His-}Fe^{2+} \rightarrow \text{His-}Fe^{2+}\text{-}CO,\,Cu_B^{1+}$$

dx.doi.org/10.1021/jp2033356 |*J. Phys. Chem. B* 2011, 115, 11455–11461

nates of heme a_3-H_2O (see below) and the ring-D prop/arginine salt bridge. Alternatively, the 385 and 392 cm^{-1} frequencies could be associated with the propionates A and D of heme a_3. In this case, the interaction between the propionate D of heme a_3 and the propionate D of heme *a* is through the Arg residue (Figure 4). This sequential or concerted H-bonded connectivity between the environments sensed by the ring-D propionate and the Arg residue in conjunction with that of the ring-A heme a_3 propionate-H_2O could have an activation energy for proton transfer.[27] This way, the above-mentioned protonic connectivity and the fast equilibrium of the water pool with bulk solvent suggest that the water pool may serve as a primary acceptor for both of the H_2O molecules formed during the catalytic turnover and pumped protons. Water molecules could act as proton carriers, transferring protons during enzymatic turnover. With the highly conserved H_2O molecule in-between propionates to act as a possible proton carrier, we can consider it to play a significant role as protonic switch, prior to its release, in the proton pumping mechanism of cytochrome oxidase. On the basis of the status of the ring-A heme a_3 propionate-H_2O site and that of the heme a_3 ring-D propionate in all structurally known heme-copper oxidases, we suggest that our data do not reflect only specific properties of the caa_3 oxidase but rather are extended to the superfamily of heme-copper oxidases.

CONCLUSIONS

In the experiments reported here we have applied our RR and "light" minus "dark" FTIR difference approach[14,15] to study the CO bound cytochrome caa_3 and to investigate the ligand dynamics subsequent to CO photolysis at room temperature, which is essential for elucidating the unique chemical mechanisms of the redox processes catalyzed by the enzyme at room temperature. The data presented here allow analysis of the general structural perturbations that are responsible for the unique conformations of heme-copper oxidases. The ligand binding conformational states of cytochrome caa_3 that we see are consistent with the α- and β-forms of heme a_3 and the α-form of Cu_B. We postulate that the conformational states resulting from changes in the distance between the iron of heme a_3 and Cu_B affect only the Fe-CO modes. Since the α- and β-forms of heme-copper oxidases have only been detected in the carbonmonoxy derivatives of heme-copper oxidases, it is tempting to propose that for the ligand (CO, O_2, and NO) binding states, the difference in the position of the copper can be detected since it interacts with CO or O_2 or NO and not with the heme directly. The complexity of the reorganization of caa_3 oxidase after the photodissociation of CO should serve as a basis for the study of other heme-copper oxidases with similar biologically active centers. These experiments are in progress in our laboratory.

AUTHOR INFORMATION

Corresponding Author

*E-mail: effiep@ucy.ac.cy.

ACKNOWLEDGMENT

We are indebted to Prof. C. Varotsis for the use of the Raman spectrometer. This work was partially supported by the University of Cyprus and the Cyprus Research Promotion Foundation grant ANAVATMISI/PAGIO/0308/14 to E.P. and by the Science Foundation Ireland BICF865 to TS.

REFERENCES

(1) Than, M. E.; Soulimane, T. *Handbook of Metalloproteins*; Wiley: New York, 2001; pp 363−378.
(2) Soulimane, T.; Buse, G.; Bourenkov, G. P.; Bartunik, H. D.; Huber, R.; Than, M. E. *EMBO J.* **2000**, *19*, 1766–1776.
(3) Giuffre, A.; Stubauer, G.; Sart, P.; Brunori, M.; Zumft, W. G.; Buse, G.; Soulimane, T. *Proc. Natl. Acad. Sci. U.S.A.* **1999**, *96*, 14718–14723.
(4) Gerscher, S.; Hildebrand, P.; Soulimane, T.; Buse, G. *Biospectroscopy* **1998**, *4*, 365–377.
(5) Ching, Y.-C.; Argade, P. V.; Rousseau, D. L. *Biochemistry* **1985**, *24*, 4938–4946.
(6) Einarsdóttir, O.; Killough, P. M.; Fee, J. A.; Woodruff, W. H. *J. Biol. Chem.* **1989**, *264*, 2405–2408.
(7) Pinakoulaki, E.; Varotsis, C. *J. Phys. Chem. B* **2008**, *112*, 1851–1857.
(8) Pinakoulaki, E.; Ohta, T.; Soulimane, T.; Kitagawa, T.; Varotsis, C. *J. Am. Chem. Soc.* **2005**, *127*, 15161–15167.
(9) Stavrakis, S.; Pinakoulaki, E.; Urbani, A.; Varotsis, C. *J. Phys. Chem. B* **2002**, *106*, 12860–12862.
(10) Varotsis, C.; Ohta, T.; Kitagawa, T.; Soulimane, T.; Pinakoulaki, E. *Angew. Chem., Int. Ed.* **2007**, *46*, 2210–2214.
(11) Daskalakis, E.; Pinakoulaki, E.; Stavrakis, S.; Varotsis, C. *J. Phys. Chem. B* **2007**, *111*, 10502–1059.
(12) Stavrakis, S.; Koutsoupakis, K.; Pinakoulaki, E.; Urbani, A.; Saraste, M.; Varotsis, C. *J. Am. Chem. Soc.* **2002**, *124*, 3814–3815.
(13) Yoshikawa, S.; Shinzawa-Itoh, K.; Nakashima, R.; Yaono, R.; Yamashita, E.; Inoue, N.; Yao, M.; Fei, M. J.; Libeu, C. P.; Mizushima, T.; Yamaguchi, H.; Tomizaki, T.; Tsukihara, T. *Science* **1998**, *280*, 1723–1729.
(14) Iwata, S.; Ostermeier, C.; Ludwig, B.; Michel, H. *Nature* **1995**, *376*, 660–669.
(15) Wikström, M.; Ribacka, C.; Molin, M.; Laakkonen, L.; Verkhovsky, M. I.; Puustinen, A. *Proc. Natl. Acad. Sci. U.S.A.* **2005**, *102*, 10478–10481.
(16) Mitchell, D. M.; Shapleigh, J. P.; Archer, A. M.; Alben, J. O.; Gennis, R. B. *Biochemistry* **1996**, *35*, 9446–9450.
(17) Wang, J.; Takahashi, S.; Hosler, P. H.; Mitchell, D. M.; Ferguson-Miller, S.; Gennis, R. B.; Rousseau, D. L. *Biochemistry* **1995**, *34*, 9819–9825.
(18) Wang, J.; Gray, K. A.; Daldal, F.; Rousseau, D. L. *J. Am. Chem. Soc.* **1995**, *117*, 9363–9364.
(19) Hosler, J. P.; Kim, Y.; Shapleigh, J.; Gennis, R. B.; Alben, J. O.; Fergusson-Miller, S.; Babcock, G. T. *J. Am. Chem. Soc.* **1994**, *116*, 5515–5516.
(20) Wang, J.; Ching, Y.-C.; Takahashi, S.; Rousseau, D. L.; Hill, J. J.; Rumbley, J.; Gennis, R. B. *J. Am. Chem. Soc.* **1993**, *115*, 3390–3391.
(21) Das, T. K.; Tomson, F. K.; Gennis, R. B.; Gordon, M.; Rousseau, D. L. *Biophys. J.* **2001**, *80*, 2039–2045.
(22) Varotsis, C.; Vamvouka, M. *J. Phys. Chem. B* **1998**, *102*, 7670–7673.
(23) Pinakoulaki, E.; Ohta, T.; Soulimane, T.; Kitagawa, T.; Varotsis, C. *J. Biol. Chem.* **2004**, *279*, 22791–22794.
(24) Ohta, T.; Pinakoulaki, E.; Soulimane, T.; Kitagawa, T.; Varotsis, C. *J. Phys. Chem. B* **2004**, *108*, 5489–5491.
(25) Koutsoupakis, K.; Stavrakis, S.; Pinakoulaki, E.; Soulimane, T.; Varotsis, C. *J. Biol. Chem.* **2002**, *277*, 32860–32866.
(26) Koutsoupakis, K.; Stavrakis, S.; Soulimane, T.; Varotsis, C. *J. Biol. Chem.* **2003**, *278*, 14893–14896.
(27) Koutsoupakis, C.; Soulimane, T.; Varotsis, C. *Biophys. J.* **2004**, *86*, 2438–2444.
(28) Koutsoupakis, C.; Soulimane, T.; Varotsis, C. *J. Biol. Chem.* **2003**, *278*, 36806–36809.
(29) Pinakoulaki, E.; Varotsis, C. *Biochemistry* **2003**, *42*, 14856–14861.
(30) Pinakoulaki, E.; Soulimane, T.; Varotsis, C. *J. Biol. Chem.* **2002**, *277*, 32867–32874.
(31) Findsen, E. W.; Centeno, J.; Babcock, G. T.; Ondrias, M. R. *J. Am. Chem. Soc.* **1987**, *109*, 5367–5372.

(32) Han, S.; Takahashi, S.; Rousseau, D. L. *J. Biol. Chem.* **2000**, *275*, 1910–1919.
(33) Pinakoulaki, E.; Vamvouka, M.; Varotsis, C. *J. Phys. Chem. B* **2003**, *107*, 9865–9868.
(34) Pinakoulaki, E.; Vamvouka, M.; Varotsis, C. *Inorg. Chem.* **2004**, *43*, 4907–4910.
(35) Oertling, W. A.; Surerus, K.; Einarsdóttir, O.; Fee, J. A.; Dyer, R. B.; Woodruff, W. *Biochemistry* **1994**, *33*, 500–507.
(36) Pinakoulaki, E.; Pfitzner, U.; Ludwig, B.; Varotsis, C. *J. Biol. Chem.* **2002**, *277*, 13563–13568.
(37) Argade, P. V.; Ching, Y. C.; Rousseau, D. L. *Science* **1984**, *225*, 329–331.
(38) Philips, G. N. J.; Teodoreo, M. L.; Li, T.; Smith, B.; Olson, J. B. *J. Phys. Chem. B* **1999**, *103*, 8817–8829.
(39) Couture, M.; Burmester, T.; Hankeln, T.; Rousseau, D. L. *J. Biol. Chem.* **2001**, *276*, 36377–36382.
(40) Dyer, R. B.; Peterson, K. A.; Stoutland, P. O.; Woodruff, W. H. *Biochemistry* **1994**, *33*, 500–507.
(41) Branden, G.; Branden, B.; Schmidt, B.; Mills, D. A.; Ferguson-Miller, S.; Brzezinski, P. *Biochemistry* **2005**, *44*, 10466–10474.
(42) Gennis, R. B. *Front. Biosci.* **2004**, *9*, 581–591.
(43) Egawa, T.; Lee, H. J.; Ji, H.; Gennis, R. B.; Yeh, S.-R.; Rousseau, D. L. *Anal. Biochem.* **2009**, *394*, 141–143.
(44) Hellwig, P.; Soulimane, T.; Mantele, W. *Eur. J. Biochem.* **2002**, *269*, 4830–4838.